International Journal of Polymeric Materials, 60:244–254, 2011

ISSN: 0091-4037 print/1563-535X online
DOI: 10.1080/00914037.2010.504175

Taylor & Francis
Taylor & Francis Group

Microstructural and Optoelectronic Studies on Polyaniline: TiO_2 Nanocomposites

S. G. Pawar,[1] S. L. Patil,[1] M. A. Chougule,[1] S. N. Achary,[2] and V. B. Patil[1]

[1]Materials Research Laboratory, School of Physical Sciences, Solapur University, Solapur, M.S., India
[2]Chemistry Division, Bhabha Atomic Research Centre, Mumbai, India

Thin films of polyaniline (PANi) and PANi: titanium oxide (TiO_2) composites have been synthesized by sol–gel spin coating technique. The TiO_2 powder of particle size 50–60 nm was synthesized by the sol–gel technique and the polyaniline was synthesized by the chemical oxidative polymerization of aniline. The composite films were characterized by X-ray diffraction (XRD), atomic force microscopy (AFM), scanning electron microscopy (SEM), Fourier transform infrared (FTIR) spectroscopy, UV-vis spectroscopy and the four-probe method. The results were compared with corresponding data on pure polyaniline films. The intensity of diffraction peaks for PANi:TiO_2 composites is lower than that for TiO_2. The characteristic FTIR peaks of pure PANi are observed to shift to a higher wavenumber in PANi:TiO_2 composite, which is attributed to the interaction of TiO_2 particles with PANi molecular chains. The resistivity measurement shows that the molecular chain constitution of polyaniline is the most important carrier in the polyaniline: nano-TiO_2 composite.

Keywords crystal structure, Fourier transform infrared spectroscopy (FTIR), polymers, sol-gel growth

Received 4 April 2010; accepted 7 June 2010.
The author (VBP) is thankful to the Department of Science and Technology, Government of India, New Delhi, for sanctioning the Fast Track Project (SR/FTP/PS-09/2007).
Address correspondence to V. B. Patil, Materials Research Laboratory, School of Physical Sciences, Solapur University, Solapur 413255, M.S., India. E-mail: drvbpatil@gmail.com

INTRODUCTION

In recent years, the development of inorganic/polymer hybrid materials on nanometer scale have been receiving significant attention due to their wide range of potential applications in optoelectronic devices [1–3] and in field effect transistors [4]. The inorganic fillers at nanoscale exhibit high surface-to-volume ratio and are thus expected to modify drastically the electrical, optical and microscopic properties of polymer. In general, the syntheses of polymer/inorganic hybrid materials have the goal of obtaining new composite materials with synergetic or complementary behaviors between the polymer and inorganic material. Polyaniline (PANi) is a widely studied polymer because of its relative ease of preparation, good environmental stability [5,6] and tunable conductivity. Nano-TiO_2 also has excellent physical and chemical properties, and it has been used in coating, sensor, solar cell and photocatalyst applications [7–10]. Thus, the preparation of polyaniline/nano-TiO_2 has been a subject of interest in many studies. Feng et al. synthesized a composite of polyaniline encapsulating nano-TiO_2 particles by in situ emulsion polymerization [11]. The authors have explained the nature of chain growth and interaction between polyaniline and nano-TiO_2 particles by Fourier transform infrared (FTIR) spectroscopic analyses [11]. Xia and Wang prepared polyaniline/nanocrystalline TiO_2 composite by ultrasonic irradiation, which is considered a novel method for the preparation of 0–3-dimensional conducting polymer/nanocrystalline composites [12]. Somani et al. reported preparation of highly piezoresistive conducting polyaniline/TiO_2 composite by the in situ deposition technique at low temperature (0°C) [13]. The technogical relevance of both conducting polyaniline and semiconducting material TiO_2 in nano form lead to the preparation of a composite of PANi and TiO_2 at molecular level interaction. Such molecular level interaction may lead to novel properties in these two dissimilar chemical components [14,15]. Sol-gel methods of preparation are more likely to have a molecular level interaction of the components in composites. To the best of our knowledge no study has been reported on the synthesis of a PANi:TiO_2 composite by the sol-gel spin coating method. In this paper we report synthesis of PANi:TiO_2 composite by the sol-gel spin coating method and their structural, morphological, optical and electrical properties.

EXPERIMENTAL

Synthesis of Polyaniline (EB)

Polyaniline was synthesized by polymerization of aniline in the presence of hydrochloric acid as a catalyst and ammonium peroxidisulphate as an oxidant by the chemical oxidative polymerization method. For the synthesis, 50 ml, 1 M HCl, and 2 ml of aniline were added together in a 250 ml beaker

with constant stirring at ≈0°C. 4.9984 g of $(NH_4)_2S_2O_8$ (ammonium per oxydisulphate) in 50 ml and 1 M HCl was suddenly added into the above solution. The temperature was maintained at ≈0°C for 5 h to complete the polymerization reaction. The precipitate obtained after the polymerization reaction was filtered. The product was washed successively by 1 M HCl followed by distilled water repeatedly until the filtrate turned colorless. Then it was re-filtered and washed once again by distilled water, to obtain the emeraldine salt form of polyaniline. To obtain the emeraldine base form of PANi, 0.1 M NH_4OH solution was added to the PANi salt and then dried at 60°C in vacuum for 24 h. This forms insulating polyaniline (EB) polymer [16].

Synthesis of Nanocrystalline TiO_2

Nanocrystalline TiO_2 is synthesized by the sol-gel method using titanium isopropoxide as a source of Ti. 3.7 ml of titanium isopropoxide was added to 40 ml of methanol and stirred vigorously at temperature 60°C for 1 h, which leads to the formation of white powder which was sintered at 700°C for 1 h to achieve formation of nanocrystalline TiO_2 of 50–60 nm size [17].

Synthesis of TiO_2–PANi Nanocomposite

The undoped polyaniline powder was dissolved in m-cresol. The solution was stirred for 11 h at room temperature and filtered. A thin film of this filtered undoped PANi was deposited by spin coating method on a glass substrate with 3000 rpm for 40 s and dried on a hot plate at 100°C for 10 min. The TiO_2 composites with undoped PANi were prepared by adding TiO_2 in different weight percentage (0–50 wt%) in a solution of undoped PANi in m-cresol followed by constant stirring for about 11 h. Thin films of the PANi-TiO_2 composite were prepared in a similar way.

Characterization and Measurement Methods

X-ray diffraction (XRD) studies were carried out using a Philips powder X-ray diffractometer (Model: PW1710). The XRD patterns were recorded in the 2θ range of 20–80° with step width 0.02° and step time 1.25 sec using CuKα radiation ($\lambda = 1.5406$ A°). The XRD patterns were analyzed by matching the observed peaks with the standard pattern provided by JCPDS file. The AFM images were recorded with a multimode scanning probe microscope system operated in tapping mode using a Being Nano-Instruments CSPM-4000. Fourier transform infrared (FTIR) spectroscopy (Model: Perkin Elmer 100) of TiO_2, PANi and PANi:TiO_2 (50%) composites was studied in the frequency range of 400–4000 cm^{-1}. Morphological study of the films of PANi and

PANi:TiO_2 composite was carried out using scanning electron microscopy (SEM Model: JEOL JSM 6360) operating at 20 kV. UV-vis spectra of the samples, which were dispersed in de-ionized water under ultrasonic action, were recorded on a Shimandzu-100 UV-vis spectrophotometer. The resistivity measurements were made on thin films using four-probe techniques. The thickness of the film was measured by using profilometry using a Dektak profilometer. The values obtained ranged between 100 and 200 nm.

RESULTS AND DISCUSSION

Figures 1 (a), (b) and (c) show XRD patterns of pure polyaniline in the emeraldine base form, PANi:TiO_2 (50%) composite and nanocrystalline titanium

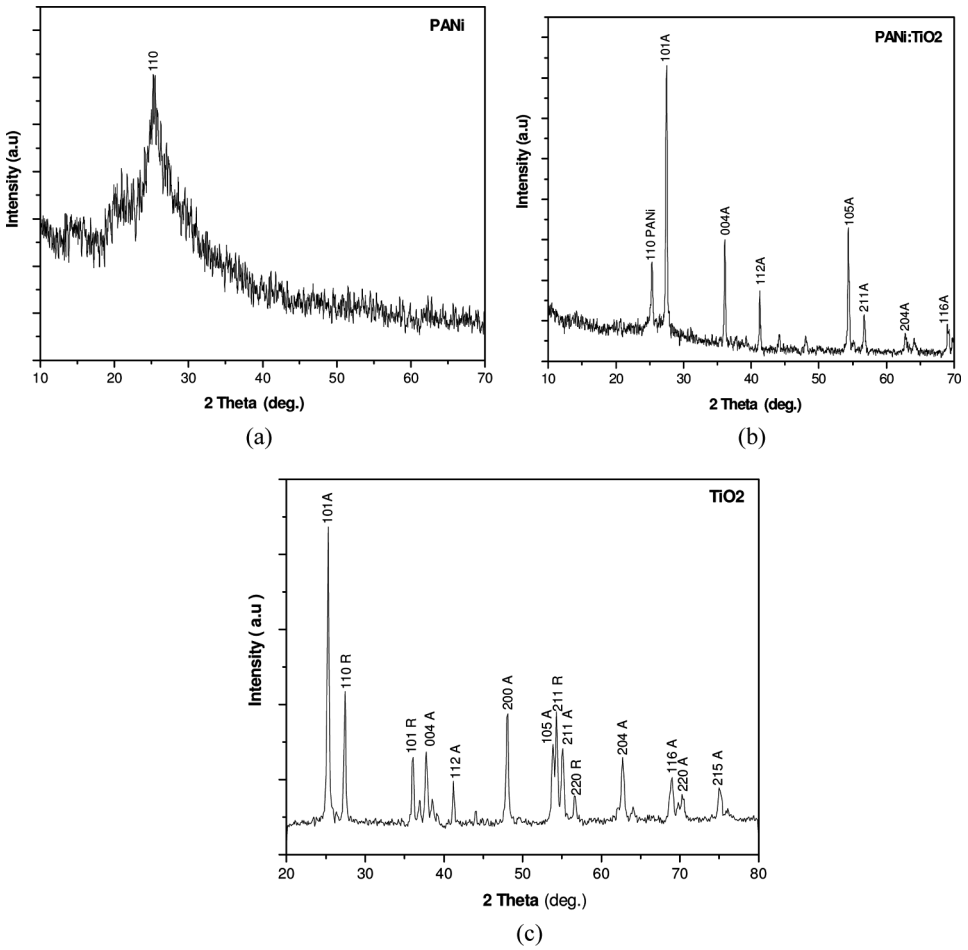

Figure 1: X-ray diffractogram of a) PANi (EB), b) PANi:TiO_2 composites, and c) TiO_2.

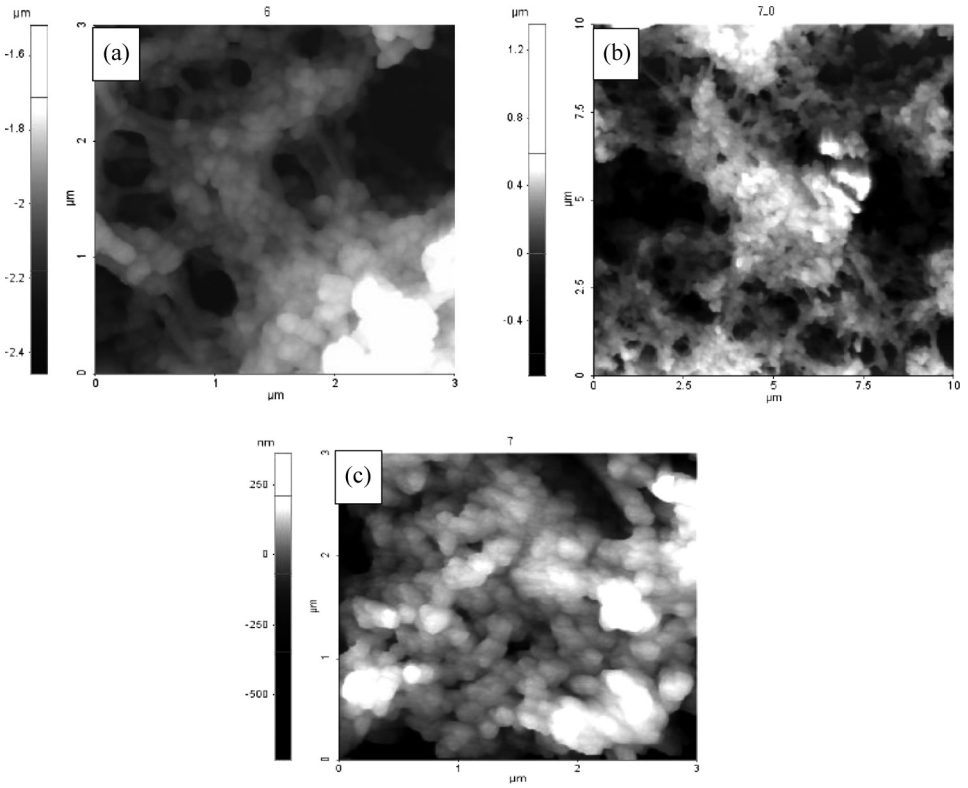

Figure 2: AFM images of a) pure PANi, b) PANi:TiO_2, and c) nano TiO_2.

oxide powder. The XRD pattern of PANi shows a broad peak at $2\theta = 25.30^\circ$ which corresponds to (110) plane [16]. Figures 1(b) and (c) show sharp and well-defined peaks, indicating the crystallinity of the synthesized materials. The observed 2θ values are consistent with the standard JCPDS data (JCPDS No. 78-1285 and 86). It could be seen that TiO_2 is formed in a mixed tetragonal anatase and rutile phases of TiO_2 (Figure 1(c)) with $a = 3.7837\,A^\circ$ and $c = 9.5087\,A^\circ$ [17]. The intensity of diffraction peaks for PANi:TiO_2 composites (Figure 1(b)) are lower than that for TiO_2. The presence of poorly crystalline PANi and the reduction of volume fraction of TiO_2 sequentially weakens diffraction peaks of TiO_2 in the composites.

AFM (tapping mode) was used to record the topography of the PANi(EB), PANi-TiO_2 and TiO_2. In this mode, the probe cantilever is oscillated at or near its resonant frequency. The surface morphologies of the PANi(EB), PANi-TiO_2 and TiO_2 exhibit notable features.

Figures 2 (a), (b), and (c) show 2D and 3D AFM images ($3\,\mu m \times 3\,\mu m$) of the PANi(EB), PANi-TiO_2 and TiO_2 films. The average surface roughnesses and peak-to-peak height values are 16, 19, 12 nm for PANi(EB), PANi-TiO_2 and

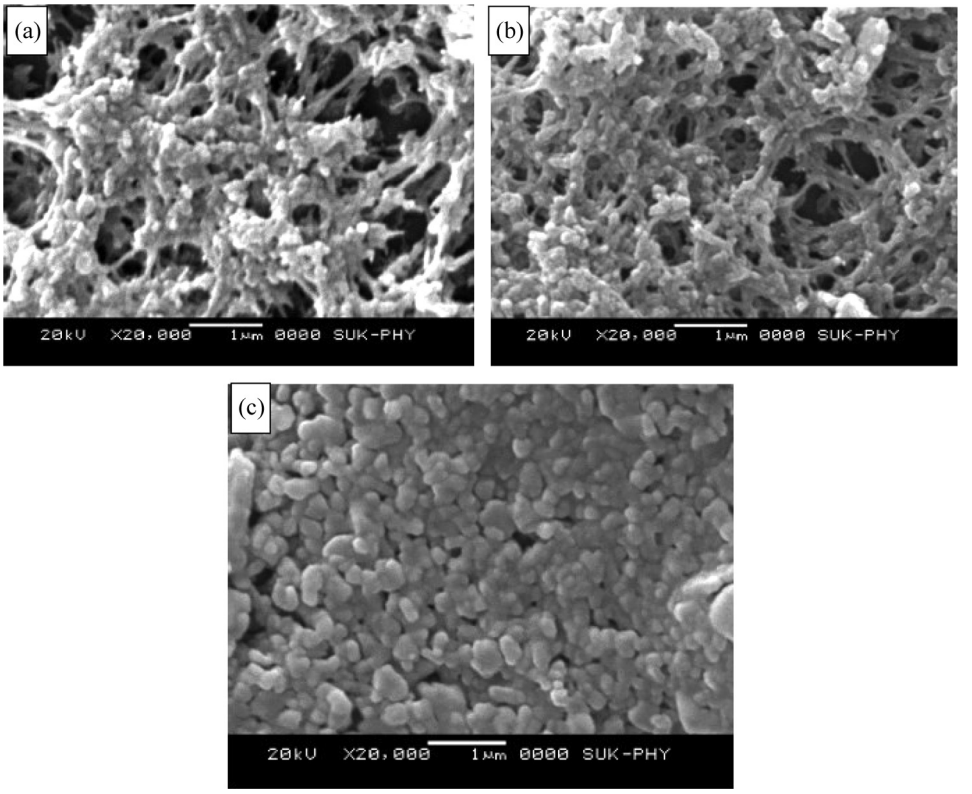

Figure 3: SEM micrographs of a) pure PANi, b) PANi:TiO_2, and c) nano TiO_2.

TiO_2. The average particle sizes of PANi(EB), PANi-TiO_2 and TiO_2 are found to be in the range of 60 nm.

Figures 3 (a), (b), and (c) show SEM micrographs of pure PANi, PANi-TiO_2 (50%) and nano TiO_2. The SEM image of the composite shows a uniform distribution of the TiO_2 particles in the PANi matrix without any agglomeration. According to the SEM images, it is observed that the nanostructured TiO_2 particles are embedded within the netlike structure built by PANi chains. It implies that the composite is highly microporous and is able to increase the liquid–solid interfacial area which provides a path for the insertion and extraction of gas molecules ions, and ensures a high reaction rate of gas sensing activity [18].

Figures 4(a), (b), and (c) show FTIR spectra of the undoped PANi, PANi-TiO_2 composite and TiO_2 nanoparticles. The origin of the vibrational bands is as follows: at 3225–3451 cm^{-1} due to the NH stretching of aromatic amines, at 2845–2914 cm^{-1} due to aromatic CH-stretching, at 504 cm^{-1} due to CH out-of-plane bending vibration. The CH out-of-plane bending mode has been used as a key to identify the type of substituted benzene. The bands

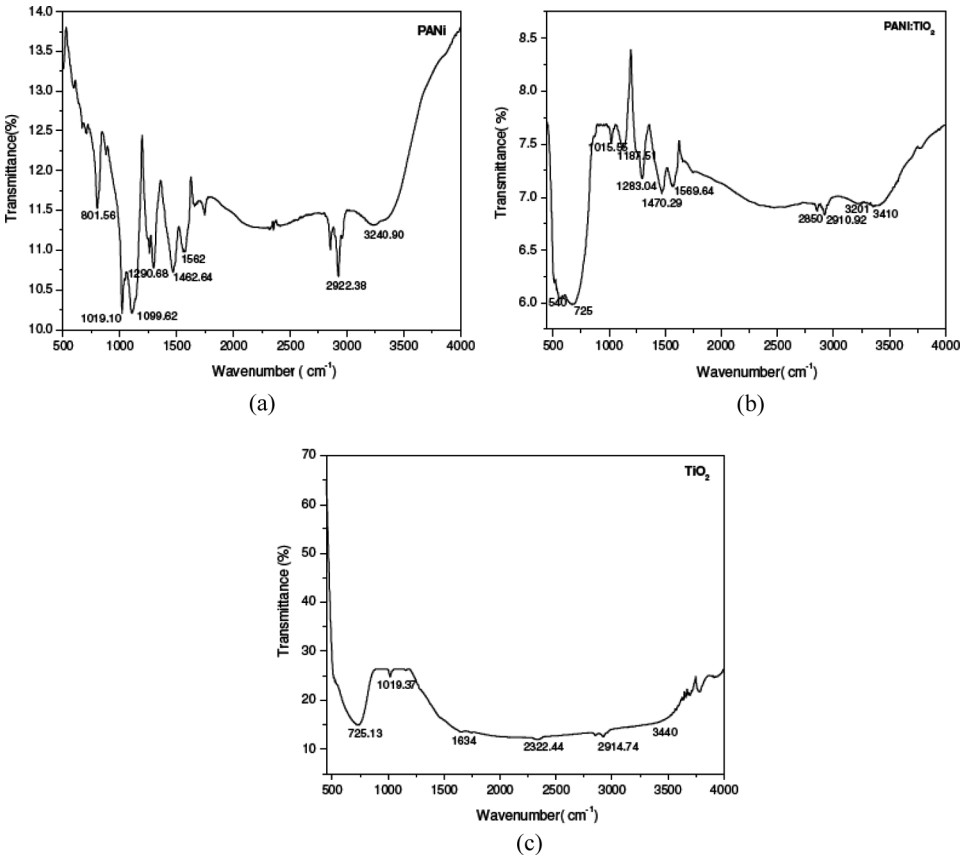

Figure 4: FTIR spectra of a) PANi (EB), b) PANi:TiO_2, and c) nano TiO_2.

at 1572 and 1489 cm^{-1} are attributed to C=N and C=C stretching modes of vibration for the quinonoid and benzenoid units of polyaniline. The peaks at 1296 and 1239 cm^{-1} are assigned to the C–N stretching mode of the benzenoid ring. The peak at 1239 cm^{-1} is the characteristic of the conducting protonated form of polyaniline. The bands in the region 1000–1115 cm^{-1} are due to in-plane bending vibration of C–H mode. The bend at 797 cm^{-1} originates from the out-of-plane C–H bending vibration. The low wavenumber region exhibits a strong vibration around 725 cm^{-1} which corresponds to the antisymmetric Ti–O–Ti mode of the titanium oxide.

UV-vis spectra of polyaniline, polyaniline/nano-TiO_2 composite and nano-TiO_2 particles are given in Figure 5. Figure 5 shows that three distinctive peaks of polyaniline appear at about 341, 441 and 924 nm, which are attributed to the π–π^*, polaron-π^* and π-polaron transition [12,18], respectively. Also from Figure 5 it can be noted that all of the characteristic peaks of nano-TiO_2 and polyaniline (EB) appear in polyaniline/nano-TiO_2 composite.

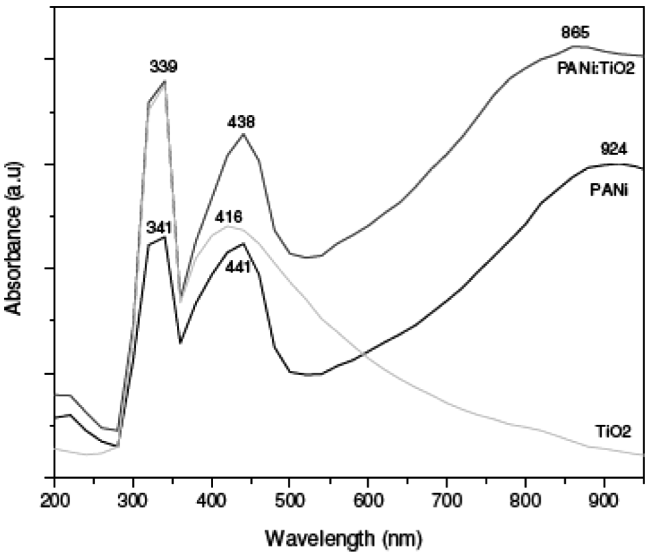

Figure 5: UV-vis absorption spectra of a) PANi (EB), b) PANi:TiO_2, and c) nano TiO_2.

Moreover, the peak at 924 nm is obviously shifted from 924 to 865 nm. This indicates that insertion of nano-TiO_2 particles has the effect of doping of the conducting polyaniline, and hence should lead to an interaction at the interface of polyaniline and nano-TiO_2 particles [12,18].

Figure 6 shows the variation of electrical resistance as a function of the temperature of the pure PANi, and Figure 7 shows the variation of electrical

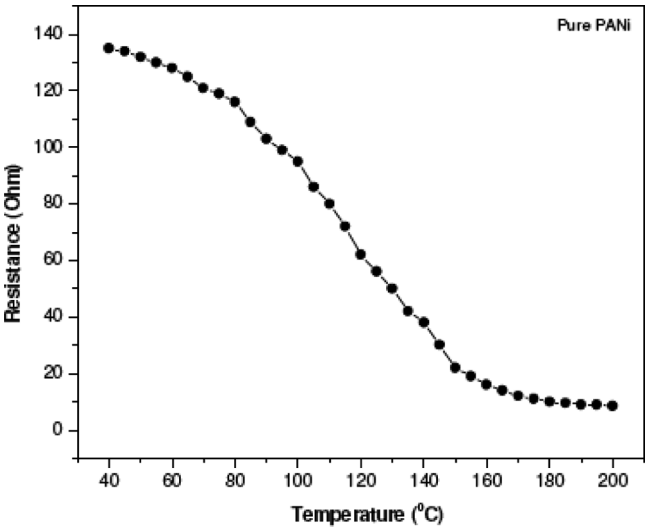

Figure 6: Resistance vs. temperature of pure PANi.

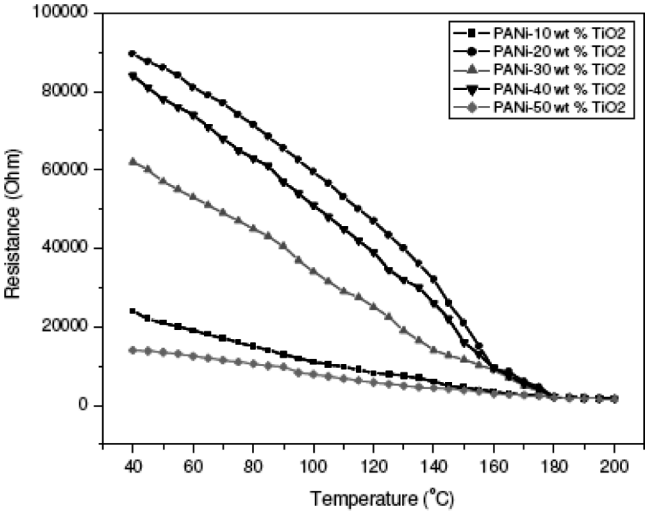

Figure 7: Resistance vs. temperature of PANi/TiO_2 composites.

resistance as a function of the temperature of pure PANi / TiO_2 composites. In both the cases it was observed that as temperature increases the electrical resistance decreases and hence conductivity increases. This suggests that the thermally activated behavior of conductivity has been confirmed. The decrease in resistance is due to the increase of efficiency of charge transfer between TiO_2 and polymer chains with an increase in temperature [19–20]. It is also suggested that the thermal curling affects the chain alignment of the polymer, which leads to the increase of conjugation length and which in turn brings about the decrease in resistance. Also, there will be molecular rearrangement on heating, which makes the molecules favorable for electron delocalization [21]. The temperature dependence of the conductivity for conducting polymers is expressed by a variable range hopping (VRH) model proposed by Mott and Davis [22]. According to this model the behavior of electronic conduction in disordered and non-metallic materials is controlled by the thermally assisted hopping of electrons between localized states near randomly distributed traps and the resistance is given by

$$R(T)\alpha \exp[-T0/T^{1/(n-1)}] \tag{1}$$

$$kT_0 = \lambda\alpha^3/\rho_0 \tag{2}$$

where, α is the coefficient of exponential decay of the localized states, ρ_0 is the density of states at the Fermi level and λ is a dimensional constant. However, many models have predicted $R = T^{-\frac{1}{2}}$.

CONCLUSION

Thin films of polyaniline, polyaniline: TiO_2 composites and nanocrystalline TiO_2 were synthesized by the sol-gel spin coating technique. X-ray investigation shows the formation of mixed anatase and rutile phases of TiO_2. The intensity of diffraction peaks for PANi:TiO_2 composites is lower than that for TiO_2. AFM images showed that the average particle sizes of PANi PANi–TiO_2 and TiO_2 are 60 nm. The SEM study of the PANi–TiO_2 composite film revealed uniform distribution of TiO_2 particles in the PANi matrix. The absorption peaks in FTIR and UV-vis spectra of PANi:TiO_2 composite film were found to shift to a higher wavenumber as compared to those observed in pure PANi. The observed shifts were attributed to the interaction between the TiO_2 particle and PANi molecular chains. The resistivity measurement shows that molecular chain constitution of polyaniline is the most important carrier in polyaniline: nano-TiO_2 composite.

REFERENCES

[1] Beek, B. W. J. E., Slooff, L. H., Wienk, M. N., Kroon, J. M., and Janseen, R. A. J. *Adv. Funct. Mater.* **15**, 1703 (2005).

[2] Sui, X. M., Shao, C. L., and Liu, Y. C. *Appl. Phys. Lett.* **87**, 113115 (2005).

[3] Olson, D. C., Piris, J., Colins, R. T., Shaheen, S. E., and Ginley, D. S. *Thin Solid Films* **496**, 26 (2006).

[4] Xu, Z. X., Roy, V. A. L., Stallinga, P., Muccini, M., Toffanin, S., Xiang, H. F., and Che, C. M. *Appl. Phys. Lett.* **90**, 223509 (2007).

[5] Gustafsson, G., Cao, Y., Treacy, G. M., Klavetter, F., Colaneri, N., and Heeger, A. *Nature* **357**, 477 (1992).

[6] Sailor, M. J., Ginsburg, E. J., Gorman, C. B., Kumar, A., Grubbs, R. H., and Lewis, N. S. *Science* **249**, 1146 (1990).

[7] Wang, X., Zu, Y., and Li, X. *Adv. Chem. Technol.* **1**, 67 (2000).

[8] Zhou, W., Sun, C. W., and Yang, Z. Z. *Acta Inorg. Mater.* **13**, 275 (1998).

[9] O'Regan, B., and Gratzel, M. *Nature* **353**, 737 (1991).

[10] Machida, M., Norimoto, K., Watanabe, T., Hashimoto, K., and Fujishima, A. *J. Mater. Sci.* **34**, 2569 (1999).

[11] Feng, W., Sun, E., Fujii, A., Wu, H. C., Niihara, K., and Yoshino, K. *Bull. Chem. Soc. Jpn.* **11**/**73**, 2627 (2000).

[12] Xia, H. S., and Wang, Q. *Chem. Mater.* **14**, 2158 (2002).

[13] Somani, P. R., Marimuthu, R., Mulik, U. P., Sainkar, S. R., and Amalnerkar, D. P. *Synthetic Met.* **106**, 45 (1999).

[14] Matsumura, M., and Ohno, T. *Adv. Mater.* **9**, 357 (1997).

[15] Yoneyama, H., Takahashi, N., and Kuwabata, S. *J. Chem. Soc. Chem. Commun.* **2**, 716 (1999).

[16] Pawar, S. G., Patil, S. L., Mane, A. T., Raut, B. T., and Patil, V. B. *Archives of Applied Science Research* **1**, 109 (2009).

[17] Pawar, S. G., Patil, S. L., Chougule, M. A., Jundale, D. M., and Patil, V. B. *J. Materials Science Materials in Electronics* (Accepted).

[18] Gospodinova, N., and Terlemezyan, L. *Prog. Polym. Sci.* **23**, 1443 (1998).

[19] Leclerc, M., D'Aparno, G., and Zotti, G. *Synth. Met.* **55**, 112 (1993).

[20] Zuo, F., Angelopoulos, M., Mac Diarmid, A. G., and Epstein, A. J. *Phys. Rev. B* **36**, 3475 (1987).

[21] Kobayashi, A., Ishikawa, H., Amano, K., Satoh, M., and Hasegawa, E. *J. Appl. Phys.* **74**, 296 (1993).

[22] Mott, N. F., and Davis, E. (1979). *Electronic Processes in Nanocrystalline Materials*, Clarendon Press, Oxford.